Symbolic Planning and Multi-Agent Path Finding in Extremely Dense Environments with Movable Obstacles

Bo Fu*, Zhe Chen*, Rahul Chandan, Alex Barbosa, Michael Caldara, Joey Durham, and Federico Pecora

Amazon Robotics
300 Riverpark Dr, North Reading, MA 01864
{bofu, zhecm, rcd, aormiga, caldaram, josepdur, fpecora}@amazon.com

Abstract

We introduce the Block Rearrangement Problem (BRaP), a challenging component of large warehouse management which involves rearranging storage blocks within dense grids to achieve a target state. We formally define the BRaP as a graph search problem. Building on intuitions from sliding puzzle problems, we propose five search-based solution algorithms, leveraging joint configuration space search, classical planning, multi-agent pathfinding, and expert heuristics. We evaluate the five approaches empirically for plan quality and scalability. Despite the exponential relation between search space size and block number, our methods demonstrate efficiency in creating rearrangement plans for deeply buried blocks in up to 80×80 grids.

1 Introduction

Amazon Robotics fulfillment centers are large warehouses that utilize robotic Automated Storage and Retrieval Systems to store inventory and fulfill customer orders. As illustrated in Figure 1, fulfillment centers store inventory items in shelves (blocks) arranged into storage grids separated by travel lanes. Robot drives can lift and move these blocks. When a station at the periphery requests a target block for item picking or stowing, robot drives move that block, transport it to the storage grid's boundary and then utilize travel lanes to bring it to the station. The system leverages dense storage grids to achieve efficient space utilization and lower fulfillment costs. This creates a challenge: target blocks may be deeply buried and obstructed by other blocks, requiring complex rearrangement plans.

We define the Block Rearrangement Problem (BRaP) as follows. Given a grid layout containing target blocks, non-target blocks, empty cells, and obstacles, as illustrated in Figure 2a, the objective is to find the lowest-cost plan to move each target block to a set of desired goal locations. Note that the non-target blocks are also referred to as movable obstacles in existing work (Papadimitriou et al. 1994). These goal locations can be either contiguous or disjoint. When goal locations are at the grid boundary, target blocks are rearranged for direct travel lane access. Alternatively, when goal locations are within the grid, target blocks are positioned for potential future access. The plan consists of block moving actions with their associated timestamps. Cost metrics can include sum of action costs, makespan, or other user-defined objectives. An example plan for the problem shown in Figure 2a is illustrated in Figure 2b.

(a) Photo

(b) Illustration diagram

Figure 1: Fulfillment center with blocks in storage grids separated by travel lanes. Target blocks marked in orange.

The Block Rearrangement Problem in dense warehouses shares fundamental structural similarities with various puzzles and real-world problems, including the sliding tile puzzle (Gozon and Yu 2024), Rush Hour puzzle (Cian et al. 2022), block relocation problem (Lu, Zeng, and Liu 2020), box world/Sokoban (Zawalski et al. 2024), parking lot rearrangement (Guo and Yu 2023), and Multi-Agent Path Finding (MAPF) (Stern et al. 2019; Li et al. 2022; Shen et al. 2023; Okumura 2023b). These problems involve rearrangement in discrete space, aiming to achieve goal configurations under movement constraints. Due to the combinatorial increase in the number of possible configurations, these

*These authors contributed equally.

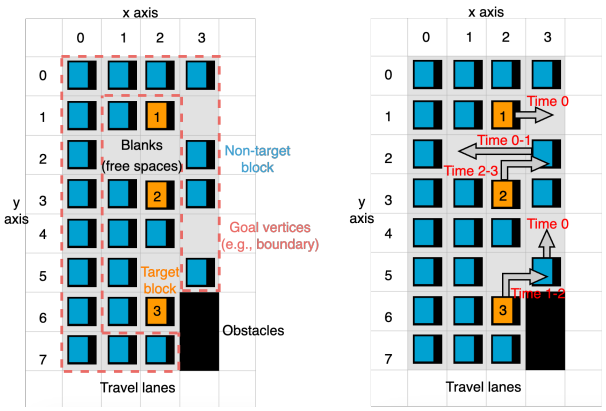

Figure 2: Block Rearrangement Problem definition.

problems are generally NP-hard (Ratner and Warmuth 1986; Flake and Baum 2002; Yu and LaValle 2013a).

This paper makes several contributions: it formally defines the Block Rearrangement Problem, establishes similarities and differences between BRaP and existing puzzles and research problems, develops five distinct solution algorithms, and evaluates their optimality and computational efficiency. Through this comprehensive analysis, we establish baseline approaches for solving BRaPs and identify directions for future research.

2 Problem Description

A BRaP is defined on a graph $G = (V, E)$ with the set of vertices V and edges $E = \{(u, v) \mid u, v \in V\}$. Let $\mathcal{I} = \{1, \cdots, n_{\mathcal{I}}\}$ denote the set of target blocks (marked in orange in Figure 2) and each target $i \in \mathcal{I}$ starts at an initial vertex $s_i \in V$ and must be moved to a set of desired goal vertices $V_i \subseteq V$. Additionally, $\mathcal{J} = \{1, \cdots, n_{\mathcal{J}}\}$ denotes non-target blocks without assigned goals. Actions A comprise a set of operations that modifies the time or location of the blocks. A path p_i for block $i \in \mathcal{I} \cup \mathcal{J}$ consists of an action sequence $(a_i^1, a_i^2, \cdots, a_i^{|p_i|}), a_i^k \in A$. Target block paths must move targets to goal vertices to be completed, while non-target block paths facilitate target block movements. A solution $P = \{p_i \mid i \in \mathcal{I} \cup \mathcal{J}\}$ to a BRaP is a set of conflict-free paths, that transition all the target blocks to their goal vertices. The objective is to find a feasible solution minimizing either sum of action costs, makespan, or other user-defined cost metrics, as detailed in Sec. 2.3.

2.1 Actions

The action set $A = \{move, wait, complete\}$ contains three actions that can be applied to the blocks, each takes one time step to execute and is associated with a corresponding cost. The action $move(i, t, u, v)$ moves block $i \in \mathcal{I} \cup \mathcal{J}$ between two adjacent vertices $(u, v) \in E$ at time step t if u is a block and v is a free space. $wait(i, t)$ forces a block to wait in place at time t. The $complete(i, t, v)$ action can only be

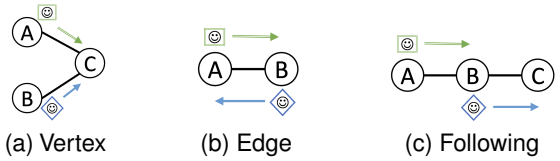

Figure 3: Three types of conflicts (Stern et al. 2019).

applied when a target block $i \in \mathcal{I}$ is at one of its goal vertices $v \in V_i$. The complete action effectively removes the block from the target block set: $\mathcal{I} \leftarrow \mathcal{I} \backslash i$.

It is important to note that, according to the above definition, the destination of a *move* action must be an empty space. We prohibit platooning, where one block closely follows another, to better align with warehouse operational constraints. Specifically, the movement must avoid the following three conflicts (Stern et al. 2019):

- *Vertex Conflict* (Figure 3a), where two blocks use the same vertex at the same timestep,
- *Edge Conflict* (Figure 3b), where two blocks use the same edge at the same timestep,
- *Following Conflict* (Figure 3c), where one block occupies a vertex that was occupied by another block in the previous time step.

2.2 Terminal State

The objective is to empty the target block set through completion actions. Three distinct completion actions are possible for target blocks. In the first case, a target block reaching the goal (e.g., the boundary) is considered rearranged and removed, converting its location to free space. In the second case, a target block becomes a non-target block upon reaching its goal location. In the third case, a target block becomes an immovable obstacle at its goal location. Each completion action corresponds to a specific practical scenario. This paper focuses on developing algorithms and conducting experiments using the third option.

2.3 Objectives and Metrics

Multiple metrics can be used to evaluate the quality of the BRaP solutions, including the number of moves of target blocks, the number of moves of non-target blocks, sum of action costs, and the makespan of the whole plan. In Block Rearrangement, we care about all of these metrics.

Let $c(a)$ denote the cost of an action $a \in A$. $c(a)$ returns the cost according to the types of the blocks and the actions. An example action cost matrix is illustrated in Table 1.

Table 1: Example action costs

Block type	*move*	*wait*	*complete*
Target	2	1	2
Non-target	2	0	N/A

The cost of a path $p_i = (a_i^1, \cdots, a_i^{|p_i|})$ is defined as:

$$c(p_i) = \sum_{k=1}^{|p_i|} c(a_i^k) \tag{1}$$

We calculate the objective metrics: composite cost of a solution $P = \{p_i \mid i \in \mathcal{I} \cup \mathcal{J}\}$ and the makespan of the solution, according to (2)-(3), respectively.

$$\text{Composite cost: } c(P) = \sum_{i \in \mathcal{I} \cup \mathcal{J}} c(p_i) \tag{2}$$

$$\text{Makespan: } c_m(P) = \max_{i \in \mathcal{I} \cup \mathcal{J}} c(p_i) \tag{3}$$

2.4 Variants of the Problem

The Problem can be extended in several ways to accommodate different operational requirements:

- *Constraint on simultaneous actions:* Limiting the number of blocks that can move concurrently to reflect real-world constraints.
- *Shared or distinct goal sets for blocks:* Blocks might have individual specific goals or share a common set of acceptable end positions.
- *Priority assignments:* Additional priority for certain blocks, ensuring critical blocks are rearranged first.

3 Related Work

As mentioned in Sec. 1, BRaP is closely related to various puzzles and research problems. Solutions to these problems have employed diverse approaches including symbolic planning (Davesa Sureda et al. 2024), search and conflict resolution (Li et al. 2022; Sharon et al. 2015; Ma et al. 2019), mixed-integer programming (Guo and Yu 2023; Lu, Zeng, and Liu 2020), boolean satisfiability (Cian et al. 2022), reinforcement learning (Shoham and Elidan 2021; Damani et al. 2021; Wang et al. 2025), and supervised learning formulations (Li et al. 2020; Jiang et al. 2025) to find low-cost plans. Given their demonstrated optimality and efficiency, we leverage symbolic planning and MAPF algorithms to develop the planning methods in this paper.

3.1 Symbolic Planning and PDDL

Symbolic planning is a model-based approach in artificial intelligence that solves decision-making problems by explicitly representing states, actions, and their transitions using symbolic logic. Planning languages like Planning Domain Definition Language (PDDL) enable the formulation of complex planning problems as structured domains, encompassing crucial elements such as initial conditions, feasible actions, and desired goal states, allowing planners to search for action sequences that achieve specified goals. PDDL has been successfully applied to various domains: modeling Rush Hour and sliding puzzles (Davesa Sureda et al. 2024), formulating Rubik's cube solutions (Muppasani, Pallagani, and Srivastava 2024), solving logistics problems for transport routing (Helmert 2009), and finding robot paths in grid worlds (Estivill-Castro and Ferrer-Mestres 2013). Symbolic representations have also proven effective in task and motion planning for robotic manipulation (Garrett et al. 2021; Silver et al. 2021). Recent work has combined the symbolic representation with deep learning and large language models to create flexible long-horizon plans (Srivastava et al. 2022; Agia et al. 2023; Lin et al. 2023). Building on this foundation, we apply symbolic planning in configuration space and PDDL descriptions to develop planning algorithms for BRaPs.

3.2 Multi-Agent Path Finding

Multi-Agent Path Finding (Stern et al. 2019) is a problem of navigating a team of agents from their start locations to goal locations without collisions. The BRaP can be modeled as a complex MAPF variant that combines elements from the classic MAPF problem (Stern et al. 2019), where agents must be moved to dedicated goal locations, the anonymous MAPF problem (Stern et al. 2019; Yu and LaValle 2013b), where goal vertices are unlabeled and are interchangeable for target blocks, and the Graph Motion Planning with Movable Obstacles problem (Papadimitriou et al. 1994), where numerous non-target blocks act as dynamic obstacles that must be moved to clear paths. But different from the anonymous MAPF problem, target blocks may been assigned distinct goal vertex sets thus goal vertices are not fully interchangeable. The BRaP is made further challenging by the high-density environment, where non-target blocks often occupy the vast majority of the workspace, and by its specific operational constraints prohibiting following. Although following conflicts are defined in the literature, most solvers ignore them and it is non-trivial to incorporate them into certain MAPF algorithms. These combined factors mean that even though powerful, state-of-the-art solvers like *LaCAM* (Okumura 2023b,a, 2024) are effective for high-density MAPF problems, they are not directly applicable to BRaPs. Therefore, building upon these advanced frameworks, we develop a MAPF-based solution tailored to the specific complexities of the BRaP.

4 Applicable Methodologies

4.1 Configuration Space Search

The BRaP can be formulated as a graph search in configuration space. Starting from an initial grid configuration, available actions transform the state until reaching a goal configuration that satisfies desired criteria. Actions at each time step represent edges that transition between neighboring configuration states. Each state comprises time, target set (vertices containing target blocks), free space set (unoccupied vertices), and completed target set (vertices containing completed target blocks).

An example graph of configuration states and actions is illustrated in Figure 4. According to the above definition, the root state in the graph is: time: 0, targets: {(2,1), (2,3), (2,6)}, free space: {(3,1), (1,2), (2,2), (2,5)}, completed target: $\emptyset$. The goal state should contain an empty target set.

The configuration space can be modified using the three actions described in Sec. 2.1. To ensure computational tractability and reduce the branching factor, we initially restrict the system to one action per time step. This restric-

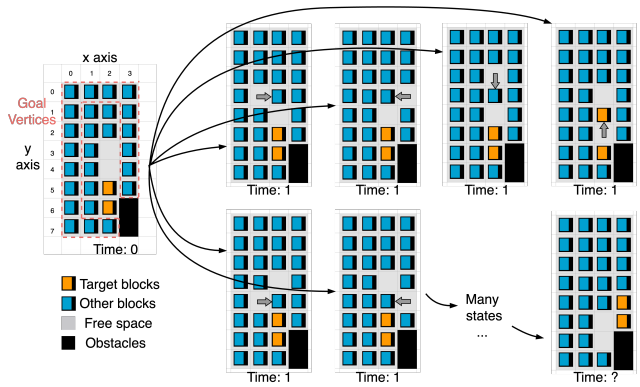

Figure 4: A graph of configuration states and actions.

tion renders the *wait* action redundant and thus disallowed. Methods supporting multiple actions at each time step will be discussed in subsequent sections.

Based on the definition of the states and actions, a configuration graph can be constructed. An example is illustrated in Figure 4. With the cost of the actions defined, graph search techniques like Dijkstra and A* algorithms can be applied to find the minimum cost path from the initial state to the goal state (where there is no longer any target blocks).

A* with an admissible heuristic function is guaranteed to be complete (always find a solution if there is) and optimal. We formulate an admissible heuristic by assuming target blocks move along least-blocking vertices, with each blocking block requiring only one *move* action for removal. The detailed heuristic formulation is presented in Appendix B.

4.2 Priority-based Configuration Space Search

In contrast to the single action per time step approach of Sec. 4.1, we now develop a formulation allowing one action per target block per time step, enabling parallel execution and reducing rearrangement makespan.

Algorithm 1 begins by assigning priorities based on block proximity to goals, as our experiments showed this produces better solutions. The priority for each target $i \in \mathcal{I}$ is determined using the heuristic $h(s, i)$ described in Appendix B, where smaller values indicate higher priorities.

The search iteratively creates rearrangement plans for individual targets while respecting plans of higher-priority blocks as constraints. For a prior plan P, the *computeConstraint*(P) function generates constraints ensuring the preconditions of higher-priority actions are satisfied. For example, if *move*(i, t, u, v) appears in P, a constraint in ξ ensures block i occupies u at time t while v remains unoccupied, and no other actions can modify these vertices at time t. The *computeConstrainedPlan*() function generates plans by pruning states violating ξ and treating prior plans as external forces, ensuring parallel executability of the resulting plans.

4.3 PDDL-based Configuration Space Search

The configuration space search can also be described using PDDL. We define five predicates: `(fre ?u)`, `(tgt ?u)`, `(blo ?u)`, `(cmp ?u)`, and `(goal ?u)`, indicating whether a vertex $u \in V$ contains a free space, target block, non-target block, completed target, or potential goal, respectively. The predicate `(adjacent ?u ?v)` denotes that vertices u and v are adjacent to each other, i.e., $(u, v) \in E$. Three actions are defined in the PDDL domain: `(move_blo ?u ?v)` and `(move_tgt ?u ?v)` for moving non-target and target blocks, respectively, and `(complete ?u)` for completion. The full PDDL domain is detailed in Appendix A.

Algorithm 1: Priority-based search

Input: Grid $G(V, E)$, target set $\mathcal{I}$, goal vertices $V_i (i \in \mathcal{I})$
$\mathcal{I}_{\text{sorted}} \leftarrow$ *computePriority*$(\mathcal{I}, V_i, V, E)$
$P \leftarrow \emptyset$ `//The initial plan`
for $i \in \mathcal{I}_{sorted}$ **do**
  $\xi \leftarrow$ *computeConstraint*(P)
  $p_i \leftarrow$ *computeConstrainedPlan*(i, V_i, V, E, P, ξ)
  $P \leftarrow P \cup p_i$
return P

In the problem file, vertices serve as objects, denoted as `node-0-0`, `node-0-1`, etc., excluding vertices containing obstacles. The initial state specifies each node's type as either `(tgt node-x-y)`, `(blo node-x-y)`, or `(fre node-x-y)`. All vertices except target blocks are marked with `(cmp node-x-y)`, and valid terminal locations are marked with `(goal node-x-y)`.

The goal state requires all vertices to be marked as `(cmp node-x-y)`, with total action cost as the optimization metric. Note that this formulation does not limit the number of simultaneous moves. However, the `fast-downward` solver used in Sec. 5 creates a totally-ordered plan where only one action is applied a time.

4.4 Heuristic Approach: Moving Along the Least Blocking Path

Given the exponentially growing configuration search space with respect to the block number, algorithms in the previous three sections do not scale efficiently to large grids with numerous target blocks. In this section, we propose a pure heuristic-based approach that moves each target along the least-blocking vertex path.

Algorithm 2 outlines the heuristic approach. The process begins by assigning priorities to target blocks using the method described in Sec. 4.2. As illustrated in Figure 5, for each target, the planner first creates a least-blocking path, $U_i = \{u_i^1, \cdots, u_i^{|U_i|}\}$, to the goal vertices. Then, for each vertex along this path, $u_i^l \in U_i$, the planner moves the closest blank to u_i^l and subsequently moves the target block to the created blank, thus generating a block movement plan. A least-blocking path is defined as the lowest-cost path where target blocks, non-target blocks, and blanks are assigned different traversal costs.

During planning, the plan for the current target i is created based on the map status where all previous target block plans have been executed. However, executing the plan for target i does not require waiting for complete execution of

Algorithm 2: Heuristic approach

Input: Grid $G(V, E)$, target set $\mathcal{I}$, goal vertices $V_i (i \in \mathcal{I})$
$\mathcal{I}_{\text{sorted}} \leftarrow$ *computePriority*$(\mathcal{I}, V_i, V, E)$
$P \leftarrow \emptyset$ //The initial plan
for $i \in \mathcal{I}_{sorted}$ **do**
  $\psi \leftarrow$ *computeVertexBlockingTime*(P)
  $U_i \leftarrow$ *leastBlockingPath*(i, V_i, V, E, P)
  $p_i \leftarrow \emptyset$
  for $u \in U_i$ **do**
    $p_i^u \leftarrow$ *moveBlankToVertex*(u, V, E, P, ψ)
    $p_i \leftarrow p_i \cup p_i^u \cup$ *move*$(i, t, u_{\text{previous}}, u)$
  $P \leftarrow P \cup p_i \cup$ *complete*(i, t, u)
return P

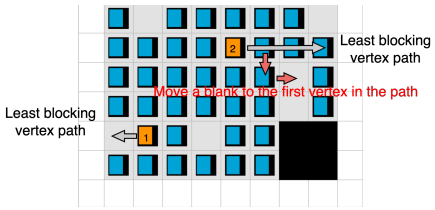

Figure 5: Move target blocks along the least blocking path.

all previous plans. Instead, it only requires waiting for the completion of plans affecting vertices that will be used by plan p_i. The function $t = \psi(u)$ takes a vertex $u \in V$ and returns this waiting time. By ensuring actions in p_i occur no earlier than times specified by ψ, the planner enables parallel execution of multiple target movements.

4.5 LaCAM-based Multi-Agent Path Finding

By discretising time into timesteps and allowing multiple blocks to move to empty vertices simultaneously in each timestep, the problem is similar to a Multi-agent Path Finding problem. With the recent advances in solving large scale and high density MAPF problems, we introduce a *Lazy Constraints Addition Search* (*LaCAM*) (Okumura 2023b,a, 2024) based algorithm to solve the BRaP in this section.

Lazy Constraints Addition Search *LaCAM* is a heuristic search algorithm that aims to rapidly find an initial solution and then continuously search for lower cost ones. The algorithm has three major components: (1) the high-level search tree, (2) the configuration generator, and (3) the low-level constraints. Similar to the Configuration Space Search presented in Sec. 4.1 and Figure 4, the high-level search component of *LaCAM* searches over the configuration space for solutions. A high-level search node n in *LaCAM* not only stores a configuration state $n.\pi$, but also low-level constraints $n.\xi$ which store spatial constraints that force the constrained blocks to perform the constrained actions. To rapidly find an initial solution, *LaCAM* searches in a way that combines *Depth-first Search* (DFS) and *Greedy Best-first Search* (GBFS).

However, unlike DFS that blindly expands from one node to the next or GBFS which applies a heuristic function to evaluate all possible successor states and expands the most

Algorithm 3: BRaP-PIBT

Input: Grid $G(V, E)$, target set $\mathcal{I}$, non-target set $\mathcal{J}$, goal vertices V_i $(i \in \mathcal{I})$, priorities ω, current states π, next states π', current temp goals g,
UpdatePriorities$(\mathcal{I}, V_i, \omega, \pi)$;
for $i \in \mathcal{I}$ **do**
  if $\pi_i = g_i$ **then** $g_i \leftarrow$ null; //Release temp goal
  $g'_i \leftarrow null$; //Next temp goal
for *each block* $k \in \mathcal{I}$ *in priority order* **do**
  if $\pi'_k = \perp$ **then** *BRaP_PIBT*(null, k) ;
BRaP_PIBT(parent, block i): **begin**
  $\pi'_i \leftarrow \pi_i$; //Default action wait
  if $i \in \mathcal{I}$ **then** $g'_i \leftarrow$ **if** g_i *is null or occupied in* g'_i **then** closest goal v, $v \notin g'$ **else** g_i ;
  if *no unused empty vertices left* **then return** true ;
  $C \leftarrow$ neighbors$(\pi_i) \cup \{\pi_i\}$; //Candidate locations
  for *each* $u \in C$ **do** *AssignPreferences*(u, i, g_i, π_i) ;
  Sort C by preference in ascending order;
  for *each candidate* $u \in C$ **do**
    if u *is occupied in* π' **then continue** ;
    if $parent \neq null$ *and* $u = \pi_i$ **then continue**;
    $j \leftarrow$ the block occupies u in π;
    if $j \neq null$ *and* $j \neq i$ **then**
      if $\pi'_j \neq \perp$ *or not BRaP_PIBT*(i, j) **then continue**;
    if $j = null$ **then** $\pi'_i \leftarrow u$; //Move if empty
    return true;
  return false;
return π', g'

promising one, *LaCAM* utilizes a configuration generator $f(n)$ to expand a given node n and generate a single successor node n' for exploration. $f(n)$ itself is a lightweight one step planner (e.g. PIBT (Okumura et al. 2022)) which suggests the most promising next state without enumerating all possible successor states.

If the new configuration, $n'.\pi$, has not yet been explored, the algorithm advances to n' and continues its deep dive in a DFS-style exploration, until a goal node is found. Conversely, if $n'.\pi$ has already been explored, the algorithm backtracks to the parent node n and grows its constraints, $n.\xi$. This addition forces the configuration generator, $f(n)$, to generate an alternative successor configuration state. $n.\xi$ grows in a brute-force manner to gradually take over the control of blocks from the configuration generator, and eventually force the exploration of all possible successor nodes of n if $f(n)$ keeps returning explored states.

BRaP-PIBT Configuration Generator With the existence of the following conflict, PIBT (Okumura et al. 2022) is no longer applicable as a configuration generator for *LaCAM* in BRaP. This is because PIBT recursively decides the actions for chains of movable blocks, while, with following conflicts, only the blocks next to empty cells are movable. The additional complexity is the BRaP has multiple goal vertices for each target block, and the configuration generator needs to decide which goal vertex to move towards. In this section, we introduce BRaP-PIBT as the configuration

generator for a *LaCAM* based MAPF solution for BRaP.

The core intuition of the BRaP-PIBT algorithm is that every block takes turns to call for empty cells in a priority-based manner, ensuring that each block is processed exactly once per step to maintain algorithmic efficiency. This approach ensures that all blocks have the opportunity to make progress toward their goals by dynamically updating their priorities. Algorithm 3 describes the process of BRaP-PIBT.

The BRaP-PIBT algorithm operates as a single-step planner that generates the next configuration state by iteratively assigning actions and temporary goals to blocks based on dynamically managed priorities. The algorithm maintains three key components: Priority Management, Recursive Planning and Temporary Goal Assignment.

Priority Management Similar to PIBT, each block i maintains a priority value ω_i that determines the order in which blocks are processed. Priorities are dynamically updated based on goal achievement and movement status. When a block i reaches any vertex in V_i, its priority is reset to a floating number in $(0, 1)$. When the block i is displaced from its goal vertices V_i, its priority is incremented by 1. This priority update process happens at the beginning of each configuration generation phase (Algorithm 3, line 2).

Recursive Planning The algorithm processes target blocks according to their priority (Algorithm 3, lines 6 - 7). For each block, it attempts to move to the most preferred adjacent location. If the desired spot is occupied, the algorithm makes a recursive call on the blocking block, finding a chain of displacement requests that reaches an empty cell (Algorithm 3, lines 8 - 23). During this process, the algorithm returns the default action *wait* if no empty vertices are left or the chain of displacement is not possible. It then identifies available neighboring vertices and sorts them based on action preference metrics. The *wait* action is only considered as a preferred option if the block is not being actively pushed by another block to find the chain (Algorithm 3 line 17). The process ensures that a block remains stationary unless a move is strategically advantageous for itself or required to accommodate another block's movement.

Temporary Goal Assignment For target blocks, BRaP-PIBT assigns temporary goals to guide them. When a block decides its action, a temporary goal is selected from the closest unassigned goal locations if the block do not have one or if its goal was taken away by a higher priority agent (Algorithm 3, line 10). The goal is released when a block reaches the assigned temporary goal (Algorithm 3, line 4).

The action preference assignment differentiates between target blocks and non-target blocks. Target blocks prioritize moves that minimize the distance to their goals, while also considering proximity to empty spaces for tie breaking. Non-target blocks focus primarily on maintaining access to empty spaces to facilitate overall system mobility. The algorithm's efficiency stems from its guarantee that each block is processed at most once per timestep. When a block is called recursively to facilitate movements, it is immediately assigned an action, thus is marked as processed.

Table 2: Experimental Setup Parameters

Parameter	**Setup**
Grid size	4x10, 6x10, 8x10, 10x10, 20x20, 40x40, 80x80
Target number	Minimum: 1 Maximum: 12.5% of grid vertices*
Blank number	Minimum: 1 Maximum: 25% of grid vertices
Goal type	Goal B: All boundary vertices Goal R1: Random goals, equal to # of targets Goal R2: Random goals, twice the # of targets
Random	10 cases for each parameter combination

*For Goal B, the maximum target number is limited to either 12.5% of $|V|$ or twice the grid height, whichever is smaller.

Integration with LaCAM The BRaP-PIBT configuration generator integrates seamlessly with the *LaCAM* framework. For each high-level node expansion, *LaCAM* uses BRaP-PIBT to generate a single successor configuration state. If explored state are generated and low-level constraints are imposed, *LaCAM* forces BRaP-PIBT to satisfy the low-level constraints by first setting the next states in π' as the constrained locations of constrained blocks, then calling BRaP-PIBT for decisions on unconstrained blocks. The combination of *LaCAM* and BRaP-PIBT enables the rapid exploration of the configuration space while still maintaining *LaCAM*'s completeness guarantee.

Anytime Improvement The other advantage of *LaCAM* is its anytime search ability. After an initial solution is found, it uses this initial solution cost as an upper bound and continues to explore the search space for a lower cost solution.

5 Results and Discussion

In this section, we evaluate the solution quality, computational time, and scalability of the algorithms proposed in Sec. 4 using an extensive set of 13,860 test cases. We systematically vary grid size, number of target blocks, number of blanks, and goal location selection methods. Table 2 lists the parameters used for generating these test cases, with representative examples visualized in Appendix D. Goal type B represents boundary vertex goals, while types R1 and R2 denote randomly selected goals, with type R1 being more restrictive in selection. Obstacles are modeled as a square region occupying 1/5 of the grid length, positioned in the bottom right corner of the grid. The PDDL formulation is solved using `fast-downward`[1]. All algorithms are evaluated on a single machine with AMD EPYC 7R13 Processor. The time limit for one test case is 10 seconds.

For each test case, success indicates finding a feasible plan within the time limit. To compare solution quality across algorithms, we establish a baseline for each test instance using the algorithm that finds the lowest final composite cost. Cost ratios are then calculated by dividing the final composite costs of other algorithms by this baseline

[1]Fast-downward: https://fast-downward.org

Table 3: Algorithm Performance Metrics Across Different Configurations Grouped by Grid Sizes and Goal Types

Groups	MAPF			Heuristic			Priority			Config			PDDL		
	Succ. Rate	Comp. Cost	Make-span	Succ. Rate	Comp. Cost	Make-span	Succ. Rate	Comp. Cost	Make-span	Succ. Rate	Comp. Cost	Make-span	Succ. Rate	Comp. Cost	Make-span
4×10	**100**	**1.00**$_{0.03}$	**1.01**$_{0.04}$	93	1.22$_{0.31}$	1.34$_{0.59}$	91	1.27$_{0.31}$	1.53$_{0.61}$	87	1.46$_{0.38}$	1.77$_{0.76}$	89	1.39$_{0.46}$	1.72$_{0.85}$
6×10	**100**	**1.01**$_{0.04}$	**1.00**$_{0.03}$	97	1.22$_{0.26}$	1.40$_{0.54}$	87	1.27$_{0.26}$	1.53$_{0.55}$	76	1.48$_{0.41}$	1.82$_{0.87}$	76	1.55$_{0.73}$	1.96$_{1.33}$
8×10	**100**	**1.01**$_{0.03}$	**1.00**$_{0.03}$	97	1.23$_{0.24}$	1.45$_{0.57}$	75	1.27$_{0.23}$	1.54$_{0.55}$	60	1.53$_{0.48}$	1.90$_{1.08}$	54	1.63$_{0.93}$	2.01$_{1.43}$
10×10	**100**	**1.00**$_{0.03}$	**1.00**$_{0.02}$	96	1.22$_{0.23}$	1.50$_{0.63}$	60	1.26$_{0.21}$	1.56$_{0.57}$	42	1.56$_{0.60}$	1.96$_{1.38}$	34	1.70$_{1.27}$	2.04$_{1.67}$
20×20	**100**	**1.01**$_{0.10}$	**1.00**$_{0.02}$	95	1.19$_{0.17}$	1.67$_{0.69}$	15	N/A	N/A	7	N/A	N/A	4	N/A	N/A
40×40	**99**	**1.04**$_{0.51}$	**1.01**$_{0.15}$	91	1.11$_{0.12}$	1.56$_{0.55}$	8	N/A	N/A	3	N/A	N/A	0	N/A	N/A
80×80	**92**	**1.04**$_{0.12}$	**1.01**$_{0.04}$	80	1.06$_{0.09}$	1.34$_{0.38}$	2	N/A	N/A	0	N/A	N/A	0	N/A	N/A
Goal B	**100**	**1.01**$_{0.03}$	**1.00**$_{0.03}$	97	1.13$_{0.14}$	1.37$_{0.44}$	56	1.20$_{0.21}$	1.45$_{0.46}$	49	1.49$_{0.47}$	1.94$_{1.05}$	45	1.51$_{0.88}$	1.89$_{1.28}$
Goal R1	**98**	**1.02**$_{0.34}$	**1.01**$_{0.10}$	82	1.27$_{0.29}$	1.63$_{0.74}$	33	1.29$_{0.28}$	1.51$_{0.64}$	22	1.35$_{0.33}$	1.46$_{0.62}$	22	1.45$_{0.82}$	1.71$_{1.16}$
Goal R2	99	**1.02**$_{0.10}$	**1.01**$_{0.04}$	**100**	1.16$_{0.22}$	1.42$_{0.52}$	56	1.29$_{0.27}$	1.56$_{0.61}$	47	1.53$_{0.48}$	1.85$_{1.02}$	44	1.57$_{0.76}$	1.96$_{1.35}$
All	**99**	**1.02**$_{0.21}$	**1.01**$_{0.06}$	93	1.18$_{0.23}$	1.46$_{0.59}$	48	1.26$_{0.26}$	1.51$_{0.57}$	39	1.48$_{0.46}$	1.81$_{1.00}$	37	1.52$_{0.82}$	1.88$_{1.29}$

*Success rate, mean composite cost ratio, and mean makespan ratio of the proposed algorithms.The subscript values are standard deviations. Smaller ratios indicate better performance. Bold values indicate the best performance across all algorithms. Ratio metrics are omitted for success rates below 20%. The algorithm abbreviations are as follows. MAPF: LaCAM-based MAPF approach, Heuristic: heuristic approach, Priority: priority-based configuration space search, Config: configuration space search, PDDL: PDDL-based configuration space search.

(resulting in ratios always greater than 1). Makespan ratios are calculated in a similar way.

Table 3 summarizes the success rate, composite cost ratio, and makespan ratio of the proposed algorithms across different grid configurations (13,860 test cases). The MAPF-based algorithm achieves the highest success rate, followed by the heuristic, priority, config, and PDDL algorithms. Only MAPF-based and heuristic algorithms successfully generate solutions for large instances. Overall, MAPF-based and heuristic algorithms achieve the lowest composite cost and makespan ratios, followed by priority, config, and PDDL approaches. Note that, the MAPF-based algorithm exhibits a higher standard deviation in composite cost on grid sizes 20×20 to 80×80 and for goal type R1. This variability indicates that for certain instances, its solutions can be substantially worse than its average performance.

As shown in Table 3, algorithm success rates decrease with increasing grid size. Only the MAPF and heuristic algorithms successfully solve large instances (grid size $\geq$ 20×20). It is important to note that the maximum number of targets increases proportionally with grid size. Notably, MAPF failures occur only when the grid size or target number exceeds computational capacity within the 10-second time limit, confirming its completeness as an algorithm - it fails only due to time constraints rather than algorithmic limitations. Table 3 also demonstrates that algorithms achieve higher success rates with goal types B and R2. Goal type R1, due to its more restrictive selection criteria, results in relatively lower success rates.

Figure 6 illustrates the time required for each algorithm to report its first solution. The MAPF and heuristic-based algorithms find solutions within 1 millisecond for over 50% of the test cases. MAPF requires more than 1 second to create a solution in less than 10% of the cases.

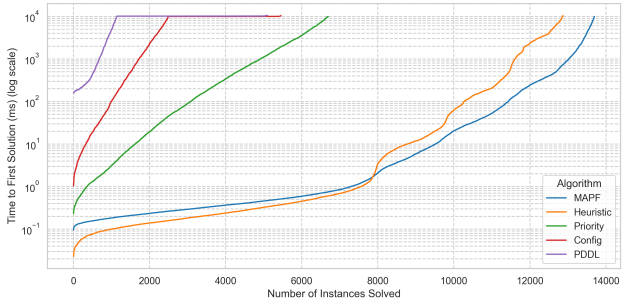

Figure 6: Time to find the first solution.

6 Conclusion

This paper formally defines the Block Rearrangement Problem and establishes its relationship to sliding puzzles. We develop five solution algorithms: configuration space search, PDDL-based planning, priority-based search, MAPF-based planning, and heuristic-based methods. Through extensive evaluation across 13,860 test cases with varying grid sizes, target numbers, and goal configurations, we evaluate the effectiveness of the proposed approaches and provide insights into their relative strengths. While most algorithms show degraded success rates with increasing grid size and more restrictive goal choices, the MAPF and heuristic-based approaches successfully solve large instances, achieving 99% and 93% success rates respectively with dense grids up to 80×80. Among the proposed methods, the MAPF and heuristic approaches demonstrate superior performance in both solution quality (composite cost and makespan) and computational efficiency, finding solutions within 1 millisecond for over 50% of test cases and within 1 second for over 90% of cases. These results establish a comprehensive baseline for solving Block Rearrangement Problems.

Based on our comprehensive analysis, future research directions include exploring various problem variants including different terminal states (where target blocks become free spaces, obstacles, or non-target blocks), additional objective functions, constraints on simultaneous actions, and practical priority requirements. Given MAPF-based approach's superior performance in this work, improving its solution quality and scalability through enhanced goal selection processes and BRaP-specific node expansion heuristics emerges as a particularly promising direction.

References

Agia, C.; Migimatsu, T.; Wu, J.; and Bohg, J. 2023. Stap: Sequencing task-agnostic policies. In *2023 IEEE International Conference on Robotics and Automation (ICRA)*, 7951–7958. IEEE.

Cian, L.; Dreossi, T.; Dovier, A.; et al. 2022. Modeling and solving the rush hour puzzle. In *CEUR Workshop Proceedings*, volume 3204, 294–306. CEUR-WS.

Damani, M.; Luo, Z.; Wenzel, E.; and Sartoretti, G. 2021. PRIMAL _2: Pathfinding via reinforcement and imitation multi-agent learning-lifelong. *IEEE Robotics and Automation Letters*, 6(2): 2666–2673.

Davesa Sureda, C.; Espasa Arxer, J.; Miguel, I.; and Villaret Auselle, M. 2024. Towards High-Level Modelling in Automated Planning. *arXiv e-prints*, arXiv–2412.

Estivill-Castro, V.; and Ferrer-Mestres, J. 2013. Pathfinding in dynamic environments with PDDL-planners. In *2013 16th International Conference on Advanced Robotics (ICAR)*, 1–7. IEEE.

Flake, G. W.; and Baum, E. B. 2002. Rush Hour is PSPACE-complete, or "Why you should generously tip parking lot attendants". *Theoretical Computer Science*, 270(1-2): 895–911.

Garrett, C. R.; Chitnis, R.; Holladay, R.; Kim, B.; Silver, T.; Kaelbling, L. P.; and Lozano-Pérez, T. 2021. Integrated task and motion planning. *Annual review of control, robotics, and autonomous systems*, 4(1): 265–293.

Gozon, M.; and Yu, J. 2024. On computing makespan-optimal solutions for generalized sliding-tile puzzles. In *Proceedings of the AAAI Conference on Artificial Intelligence*, volume 38, 10288–10296.

Guo, T.; and Yu, J. 2023. Toward efficient physical and algorithmic design of automated garages. In *2023 IEEE International Conference on Robotics and Automation (ICRA)*, 1364–1370. IEEE.

Helmert, M. 2009. Concise finite-domain representations for PDDL planning tasks. *Artificial Intelligence*, 173(5-6): 503–535.

Jiang, H.; Wang, Y.; Veerapaneni, R.; Duhan, T.; Sartoretti, G.; and Li, J. 2025. Deploying Ten Thousand Robots: Scalable Imitation Learning for Lifelong Multi-Agent Path Finding. In *2025 IEEE International Conference on Robotics and Automation (ICRA)*. IEEE.

Li, J.; Chen, Z.; Harabor, D.; Stuckey, P. J.; and Koenig, S. 2022. MAPF-LNS2: Fast repairing for multi-agent path finding via large neighborhood search. In *Proceedings of the AAAI Conference on Artificial Intelligence*, volume 36, 10256–10265.

Li, Q.; Gama, F.; Ribeiro, A.; and Prorok, A. 2020. Graph neural networks for decentralized multi-robot path planning. In *2020 IEEE/RSJ international conference on intelligent robots and systems (IROS)*, 11785–11792. IEEE.

Lin, K.; Agia, C.; Migimatsu, T.; Pavone, M.; and Bohg, J. 2023. Text2motion: From natural language instructions to feasible plans. *Autonomous Robots*, 47(8): 1345–1365.

Lu, C.; Zeng, B.; and Liu, S. 2020. A study on the block relocation problem: Lower bound derivations and strong formulations. *IEEE Transactions on Automation Science and Engineering*, 17(4): 1829–1853.

Ma, H.; Harabor, D.; Stuckey, P. J.; Li, J.; and Koenig, S. 2019. Searching with consistent prioritization for multi-agent path finding. In *Proceedings of the AAAI conference on artificial intelligence*, volume 33, 7643–7650.

Muppasani, B.; Pallagani, V.; and Srivastava, B. 2024. Solving the Rubik's Cube with a PDDL Planner. *ICAPS 2024 System's Demonstration track*.

Okumura, K. 2023a. Improving LaCAM for scalable eventually optimal multi-agent pathfinding. In *Proceedings of the Thirty-Second International Joint Conference on Artificial Intelligence*, 243–251.

Okumura, K. 2023b. Lacam: Search-based algorithm for quick multi-agent pathfinding. In *Proceedings of the AAAI Conference on Artificial Intelligence*, volume 37, 11655–11662.

Okumura, K. 2024. Engineering LaCAM*: Towards Real-time, Large-scale, and Near-optimal Multi-agent Pathfinding. In *Proceedings of the 23rd International Conference on Autonomous Agents and Multiagent Systems*, 1501–1509.

Okumura, K.; Machida, M.; Défago, X.; and Tamura, Y. 2022. Priority inheritance with backtracking for iterative multi-agent path finding. *Artificial Intelligence*, 310: 103752.

Papadimitriou, C. H.; Raghavan, P.; Sudan, M.; and Tamaki, H. 1994. Motion planning on a graph. In *Proceedings 35th Annual Symposium on Foundations of Computer Science*, 511–520. IEEE.

Ratner, D.; and Warmuth, M. 1986. Finding a shortest solution for the N x N extension of the 15-puzzle is intractable. In *Proceedings of the Fifth AAAI National Conference on Artificial Intelligence*, 168–172.

Sharon, G.; Stern, R.; Felner, A.; and Sturtevant, N. R. 2015. Conflict-based search for optimal multi-agent pathfinding. *Artificial intelligence*, 219: 40–66.

Shen, B.; Chen, Z.; Li, J.; Cheema, M. A.; Harabor, D. D.; and Stuckey, P. J. 2023. Beyond Pairwise Reasoning in Multi-Agent Path Finding. In *International Conference on Automated Planning and Scheduling*.

Shoham, Y.; and Elidan, G. 2021. Solving sokoban with forward-backward reinforcement learning. In *Proceedings of the International Symposium on Combinatorial Search*, volume 12, 191–193.

Silver, T.; Chitnis, R.; Tenenbaum, J.; Kaelbling, L. P.; and Lozano-Pérez, T. 2021. Learning symbolic operators for task and motion planning. In *2021 IEEE/RSJ International Conference on Intelligent Robots and Systems (IROS)*, 3182–3189. IEEE.

Srivastava, S.; Li, C.; Lingelbach, M.; Martín-Martín, R.; Xia, F.; Vainio, K. E.; Lian, Z.; Gokmen, C.; Buch, S.; Liu, K.; et al. 2022. Behavior: Benchmark for everyday household activities in virtual, interactive, and ecological environments. In *Conference on robot learning*, 477–490. PMLR.

Stern, R.; Sturtevant, N. R.; Felner, A.; Koenig, S.; Ma, H.; Walker, T. T.; Li, J.; Atzmon, D.; Cohen, L.; Kumar, T. K. S.; Boyarski, E.; and Barták, R. 2019. Multi-Agent Pathfinding: Definitions, Variants, and Benchmarks. *ArXiv*, abs/1906.08291.

Wang, Y.; Duhan, T.; Li, J.; and Sartoretti, G. 2025. LNS2+ RL: Combining multi-agent reinforcement learning with large neighborhood search in multi-agent path finding. In *Proceedings of the AAAI Conference on Artificial Intelligence*, volume 39, 23343–23350.

Yu, J.; and LaValle, S. 2013a. Structure and intractability of optimal multi-robot path planning on graphs. In *Proceedings of the AAAI Conference on Artificial Intelligence*, volume 27, 1443–1449.

Yu, J.; and LaValle, S. M. 2013b. Multi-agent path planning and network flow. In *Algorithmic Foundations of Robotics X: Proceedings of the Tenth Workshop on the Algorithmic Foundations of Robotics*, 157–173. Springer.

Zawalski, M.; Góral, G.; Tyrolski, M.; Wiśnios, E.; Budrowski, F.; Cygan, M.; Kuciński, Ł.; and Miłoś, P. 2024. What Matters in Hierarchical Search for Combinatorial Reasoning Problems? *arXiv preprint arXiv:2406.03361*.

A PDDL Domain

```
(define
    (domain block-rearrangement)
    (:requirements :strips :action-costs)
    (:predicates
        (tgt ?loc)
        (fre ?loc)
        (blo ?loc)
        (cmp ?loc)
        (goal ?loc)
        (adjacent ?loc1 ?loc2)
    )
    (:action slide_blo
        :parameters (?from ?to)
        :precondition  (and (blo ?from) (fre ?to) (
            adjacent ?from ?to))
        :effect (and
                (not (blo ?from))
                (blo ?to)
                (not (fre ?to))
                (fre ?from)
                )
    )
    (:action slide_tgt
        :parameters (?from ?to)
        :precondition  (and (tgt ?from) (fre ?to) (
            adjacent ?from ?to))
        :effect (and
                (not (tgt ?from))
                (tgt ?to)
                (not (fre ?to))
                (fre ?from)
                (cmp ?from)
                (not (cmp ?to))
                )
    )
    (:action complete
        :parameters (?loc)
        :precondition  (and (goal ?loc) (tgt ?loc))
        :effect (and
                (not (tgt ?loc))
                (cmp ?loc)
                )
    )
)
```

B Admissible Heuristic for Configuration Space Search

A admissible heuristic is formulated by assuming target blocks move along least-blocking vertices and each blocking block can be cleared using only one *move* action. Using the example state s in Figure 7, we demonstrate the heuristic value calculation for two target blocks. We calculate a lower bound cost for moving each target to its goal set. Target 1 requires: an initial *move*, clearing the block at (3, 4) (minimum one *move*), a final *move*, and a *complete* action. Therefore, the lower bound cost for target 1 is $h(s,1) = c_{move} + c_{move} + c_{move} + c_{complete} = 3c_{move} + c_{complete}$. Similarly, the movement of target 2 to the goals requires two *move* actions and one *complete* action, yielding a lower bound cost of $h(s,2) = c_{move} + c_{move} + c_{complete} = 2c_{move} + c_{complete}$. Since actions moving one target can benefit the movement of other targets, we estimate a joint cost lower bound by averaging individual target costs. Thus, for this example: $h(s) = (h(s,1) + h(s,2))/2 = [(3c_{move} + c_{complete}) + (2c_{move} + c_{complete})]/2 = 2.5c_{move} + c_{complete}$.

Let the lowest action cost to move the targets to the goals be $h^*(s)$.

Claim 1: $h(s)$ is admissible: $h(s) \leq h^*(s)$.

Proof. Let the lowest cost to move each target $i \in \mathcal{I}$ to their goal vertices be $h^*(s,i)$. By definition, $h(s,i)$ underestimates the cost to move target i. Therefore, $h(s,i) \leq h^*(s,i) \leq h^*(s)$. Therefore, $h(s) = \frac{1}{|\mathcal{I}|}\sum_{i\in\mathcal{I}} h(s,i) \leq \frac{1}{|\mathcal{I}|}|\mathcal{I}|h^*(s) = h^*(s)$. □

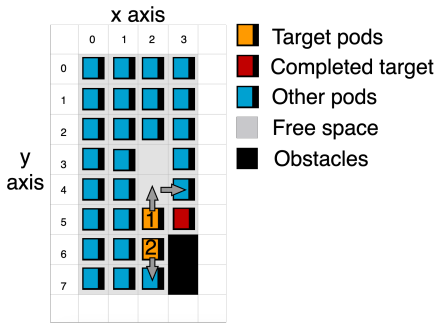

Figure 7: Illustration of the formulated heuristic. The goal of the target blocks is the boundary.

C Completeness Guarantee for LaCAM-based MAPF Approach

LaCAM is a complete algorithm for MAPF problems. It guarantees that if a MAPF prolem is solvable, the algorithm finds and returns the solution. For BRaP, the *LaCAM*-based planner modified *LaCAM* for MAPF by replacing PIBT with BRaP-PIBT and enforcing constraints on blocks next to empty vertices only. The high-level search framework is unchanged.

Claim 2: *LaCAM*-based planner is complete, which returns a solution for solvable BRaP problem.

Proof. Following (Okumura 2023b), the search space is finite and the number of configuration states is $|V|^{|\mathcal{I}\cup\mathcal{J}|}$. Since the low-level constraints enumerate all possible combinations of movements for all blocks, it generates all possible configuration states that connects to a high-level node's configuration state. Consequently, all reachable configuration states from the start configuration state are explored. □

D Example Test Cases

Example test cases are illustrated in Figure 9.

E Additional Results

This section provides supplementary experimental results to Sec. 5. Table 6 illustrate the detailed success rates, average composite Cost Ratios, and makespan ratios. The results are grouped by goal types, number of target blocks, and grid sizes.

Table 4-5 presents pairwise comparisons between algorithms. Each cell shows the average composite cost and makespan ratios for co-solvable instances between row and column algorithms (row algorithm cost divided by column algorithm cost). These comparisons confirm the solution quality ranking observed in Table 3 and Table 6. Figure 8a visualizes the composite cost ratios across all 13,860 test instances, with each instance represented by a single dot. Consistent with the results in Table 3, failure rates increase with grid size and number of target blocks. The Cost Ratios among algorithms typically range between 1 and 10 relative to the best performer. Figure8b - 8d further break Figure 8a down by goal types.

Table 7 demonstrated the anytime improvement ability of the *LaCAM*-based MAPF approach. It shows the composite cost ratio of the first solution found by the algorithm, the average time on when the first solution was found, and the composite cost of the final solution found by the 10 seconds timelimit.

Overall, MAPF achieves the lowest composite costs and makespan, followed by heuristic, priority, config, and PDDL-based approaches.

Table 4: Pairwise comparison between the final cost on co-solvable instances.

	MAPF	Heuristic	Priority	Config	PDDL
MAPF	1	0.861	0.800	0.682	0.661
Heuristic	1.162	1	0.948	0.798	0.774
Priority	1.249	1.055	1	0.841	0.842
Config	1.467	1.253	1.189	1	0.990
PDDL	1.513	1.292	1.188	1.010	1

Table 5: Pairwise comparison between the makespan on co-solvable instances.

	MAPF	Heuristic	Priority	Config	PDDL
MAPF	1	0.686	0.667	0.556	0.535
Heuristic	1.457	1	0.875	0.712	0.69
Priority	1.499	1.143	1	0.813	0.808
Config	1.8	1.404	1.231	1	0.978
PDDL	1.87	1.449	1.238	1.022	1

E.1 Distinct Goal Location Sets for Each Target Block

Table 8 shows additional experiment results on instances that each target block has individually random sampled goal location set. In this benchmark set, we generated 4620 test cases, with grid size, target number and blank number varies in the same range shown in Table 2. But for each target block, we independently sample 5 potential goal locations. This means the goal location sets between target blocks may be disjoint, overlapping, or exactly the same.

These uniquely challenging instances are only supported by the *LaCAM*-based MAPF approach, which is able to dynamically decides the final goal location during the search process. Table 8 shows that it achieves a high success rate, computes first solution rapidly, and improves the final solution cost in an anytime manner.

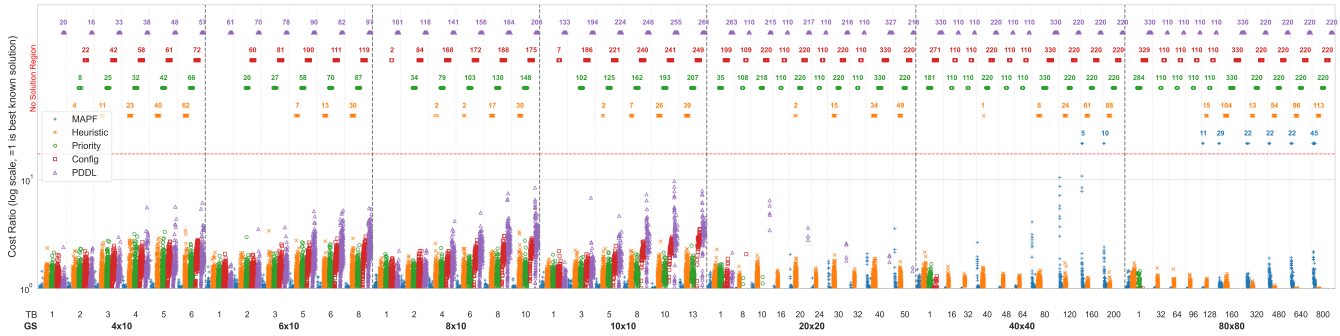

(a) On all goal types

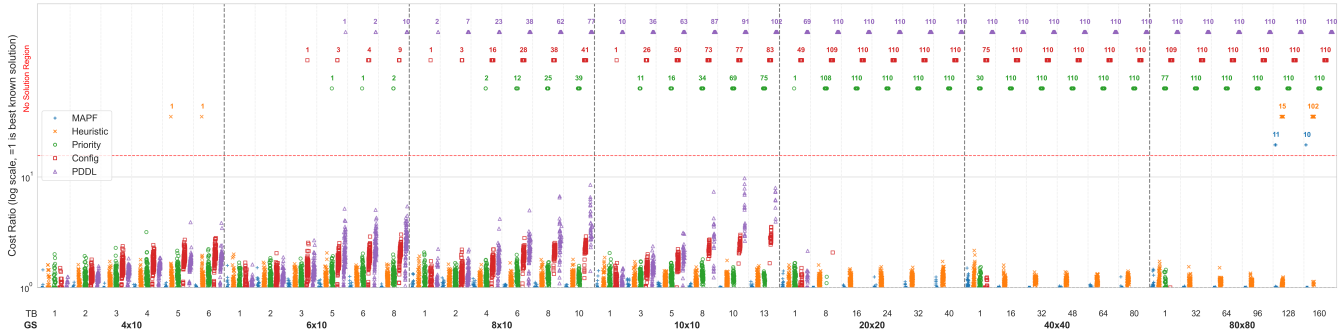

(b) On goal type B

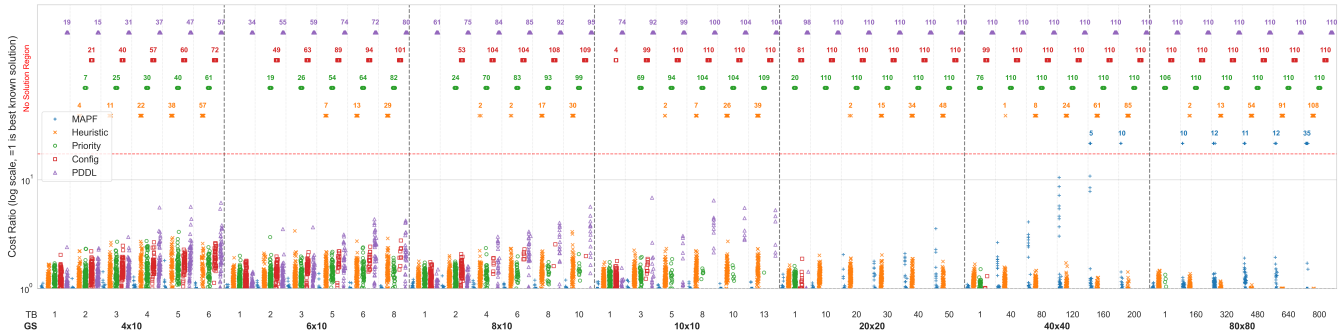

(c) On goal type R1

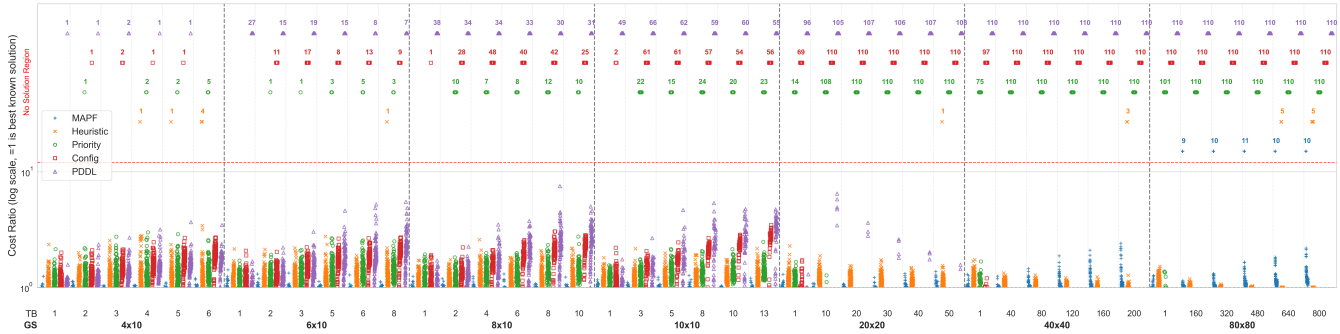

(d) On goal type R2

Figure 8: Composite Cost Ratio for each instance, grouped by number of target blocks (TB) and grid size (GS). The number and dots in the no solution region shows how many instances are unsolved for each algorithm in each group.

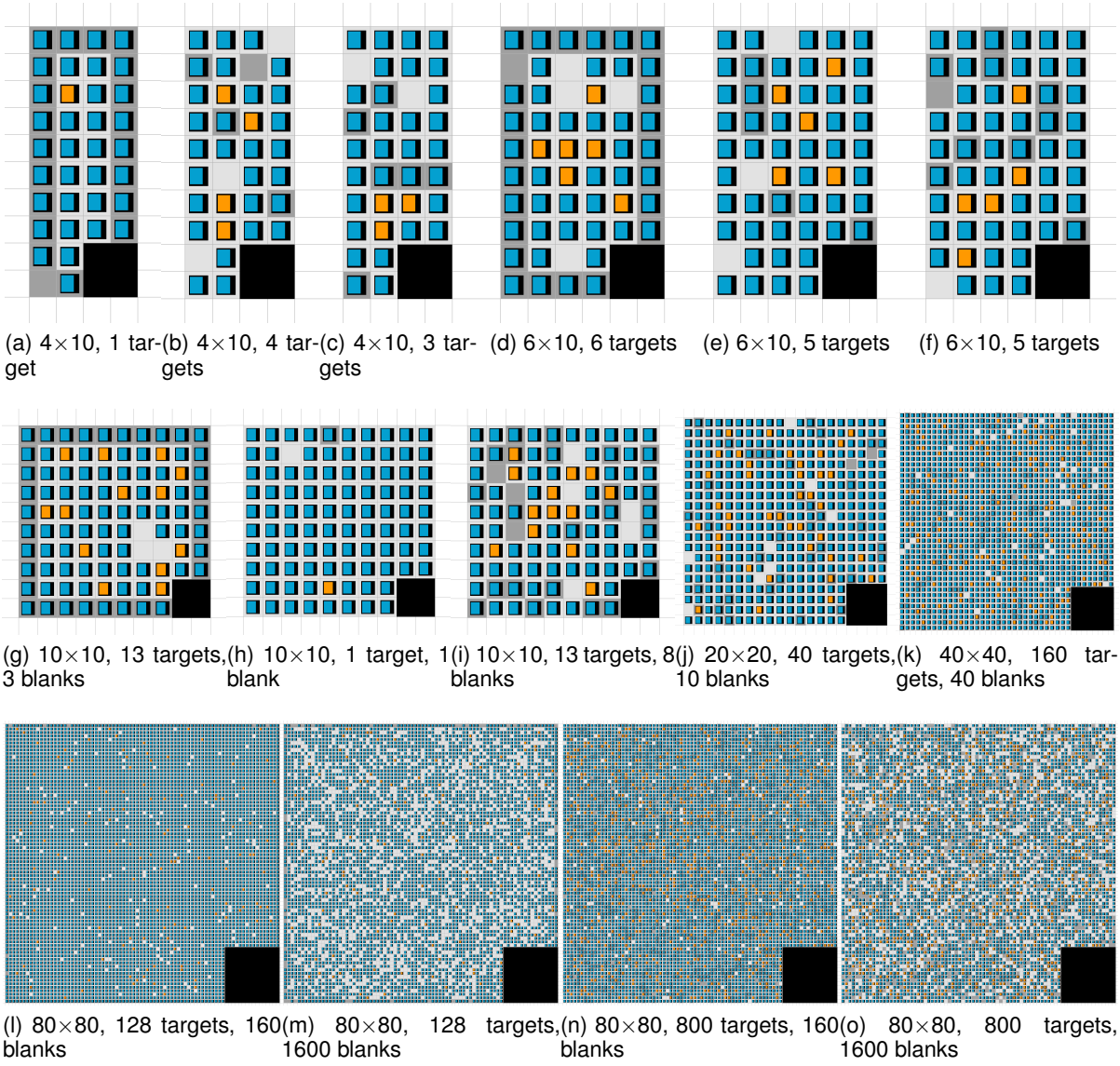

Figure 9: Example test cases. Dark gray vertices indicate the goals for the target blocks. Black vertices indicate obstacles.

Table 6: Detailed success rate, average composite cost ratio, and average makespan ratio comparison, grouped by grid size (GS) and number of target blocks (TB).

Groups		MAPF			Heuristic			Priority			Config			PDDL		
GS	TB	Succ. Rate	Comp. Cost Ratio	Make-span Ratio	Succ. Rate	Comp. Cost Ratio	Make-span Ratio	Succ. Rate	Comp. Cost Ratio	Make-span Ratio	Succ. Rate	Comp. Cost Ratio	Make-span Ratio	Succ. Rate	Comp. Cost Ratio	Make-span Ratio
4×10	1	100	$1.00_{0.03}$	$1.00_{0.03}$	100	$1.11_{0.18}$	$1.12_{0.17}$	100	$1.12_{0.19}$	$1.14_{0.21}$	100	$1.11_{0.19}$	$1.13_{0.19}$	94	$1.04_{0.11}$	$1.07_{0.16}$
	2	100	$1.00_{0.02}$	$1.01_{0.03}$	99	$1.18_{0.22}$	$1.22_{0.34}$	98	$1.20_{0.23}$	$1.35_{0.39}$	93	$1.29_{0.21}$	$1.46_{0.32}$	95	$1.22_{0.20}$	$1.42_{0.31}$
	3	100	$1.00_{0.03}$	$1.01_{0.04}$	97	$1.24_{0.29}$	$1.35_{0.52}$	92	$1.29_{0.30}$	$1.57_{0.54}$	87	$1.44_{0.26}$	$1.77_{0.49}$	90	$1.37_{0.25}$	$1.70_{0.44}$
	4	100	$1.00_{0.02}$	$1.01_{0.04}$	93	$1.27_{0.38}$	$1.43_{0.69}$	90	$1.33_{0.37}$	$1.68_{0.64}$	82	$1.58_{0.28}$	$2.06_{0.57}$	88	$1.52_{0.45}$	$2.01_{0.75}$
	5	100	$1.01_{0.05}$	$1.01_{0.05}$	88	$1.29_{0.36}$	$1.48_{0.72}$	87	$1.39_{0.34}$	$1.84_{0.66}$	82	$1.71_{0.32}$	$2.29_{0.71}$	85	$1.64_{0.49}$	$2.19_{0.87}$
	6	100	$1.00_{0.02}$	$1.01_{0.03}$	81	$1.28_{0.35}$	$1.52_{0.73}$	80	$1.38_{0.29}$	$1.87_{0.67}$	78	$1.87_{0.37}$	$2.57_{0.84}$	83	$1.78_{0.59}$	$2.46_{1.04}$
6×10	1	100	$1.01_{0.05}$	$1.00_{0.03}$	100	$1.15_{0.20}$	$1.13_{0.17}$	100	$1.13_{0.18}$	$1.15_{0.20}$	100	$1.13_{0.19}$	$1.14_{0.20}$	82	$1.05_{0.11}$	$1.06_{0.12}$
	2	100	$1.01_{0.05}$	$1.01_{0.04}$	100	$1.17_{0.22}$	$1.25_{0.35}$	94	$1.21_{0.23}$	$1.37_{0.41}$	82	$1.29_{0.21}$	$1.49_{0.34}$	79	$1.23_{0.24}$	$1.45_{0.38}$
	3	100	$1.01_{0.03}$	$1.01_{0.05}$	100	$1.21_{0.26}$	$1.34_{0.46}$	92	$1.27_{0.23}$	$1.54_{0.44}$	75	$1.46_{0.27}$	$1.75_{0.48}$	76	$1.40_{0.33}$	$1.76_{0.56}$
	5	100	$1.01_{0.03}$	$1.00_{0.03}$	98	$1.26_{0.27}$	$1.51_{0.55}$	82	$1.36_{0.28}$	$1.78_{0.56}$	70	$1.67_{0.30}$	$2.28_{0.64}$	73	$1.79_{0.65}$	$2.49_{1.14}$
	6	100	$1.00_{0.03}$	$1.00_{0.02}$	96	$1.27_{0.25}$	$1.57_{0.61}$	79	$1.37_{0.28}$	$1.82_{0.62}$	66	$1.78_{0.34}$	$2.52_{0.80}$	75	$1.99_{0.76}$	$2.80_{1.28}$
	8	100	$1.00_{0.01}$	$1.00_{0.01}$	91	$1.30_{0.30}$	$1.71_{0.64}$	74	$1.35_{0.24}$	$1.84_{0.55}$	64	$1.96_{0.36}$	$2.90_{0.83}$	71	$2.28_{0.82}$	$3.31_{1.57}$
8×10	1	100	$1.01_{0.04}$	$1.00_{0.03}$	100	$1.14_{0.18}$	$1.13_{0.17}$	100	$1.16_{0.21}$	$1.17_{0.23}$	99	$1.14_{0.19}$	$1.15_{0.20}$	69	$1.07_{0.18}$	$1.07_{0.14}$
	2	100	$1.01_{0.03}$	$1.01_{0.05}$	100	$1.18_{0.19}$	$1.23_{0.29}$	90	$1.22_{0.19}$	$1.38_{0.35}$	75	$1.32_{0.24}$	$1.46_{0.35}$	65	$1.26_{0.23}$	$1.46_{0.35}$
	4	100	$1.01_{0.03}$	$1.00_{0.02}$	99	$1.24_{0.23}$	$1.45_{0.48}$	76	$1.30_{0.22}$	$1.61_{0.46}$	49	$1.54_{0.26}$	$1.98_{0.49}$	57	$1.61_{0.51}$	$2.11_{0.83}$
	6	100	$1.01_{0.03}$	$1.00_{0.02}$	99	$1.25_{0.24}$	$1.53_{0.54}$	69	$1.32_{0.22}$	$1.77_{0.55}$	48	$1.84_{0.31}$	$2.72_{0.70}$	53	$1.99_{0.64}$	$2.75_{1.10}$
	8	100	$1.00_{0.02}$	$1.00_{0.02}$	95	$1.27_{0.25}$	$1.71_{0.65}$	61	$1.35_{0.23}$	$1.91_{0.58}$	43	$2.03_{0.34}$	$3.17_{0.80}$	44	$2.36_{1.01}$	$3.26_{1.62}$
	10	100	$1.00_{0.02}$	$1.00_{0.01}$	91	$1.29_{0.31}$	$1.77_{0.71}$	55	$1.33_{0.24}$	$1.92_{0.62}$	47	$2.22_{0.36}$	$3.50_{0.91}$	38	$2.72_{1.24}$	$3.69_{1.45}$
10×10	1	100	$1.01_{0.04}$	$1.00_{0.04}$	100	$1.14_{0.18}$	$1.12_{0.14}$	100	$1.15_{0.18}$	$1.15_{0.18}$	98	$1.13_{0.18}$	$1.14_{0.18}$	60	$1.06_{0.13}$	$1.06_{0.12}$
	3	100	$1.01_{0.03}$	$1.01_{0.03}$	100	$1.21_{0.21}$	$1.33_{0.39}$	69	$1.25_{0.19}$	$1.49_{0.44}$	44	$1.45_{0.23}$	$1.73_{0.49}$	41	$1.43_{0.56}$	$1.81_{0.71}$
	5	100	$1.01_{0.02}$	$1.00_{0.02}$	99	$1.22_{0.21}$	$1.47_{0.49}$	62	$1.30_{0.22}$	$1.67_{0.50}$	33	$1.68_{0.25}$	$2.35_{0.62}$	32	$1.72_{0.64}$	$2.22_{1.03}$
	8	100	$1.00_{0.02}$	$1.00_{0.02}$	98	$1.26_{0.25}$	$1.64_{0.66}$	51	$1.32_{0.19}$	$1.85_{0.53}$	27	$2.13_{0.28}$	$3.32_{0.74}$	25	$2.51_{1.15}$	$3.22_{1.48}$
	10	100	$1.00_{0.01}$	$1.00_{0.00}$	92	$1.26_{0.23}$	$1.73_{0.66}$	42	$1.34_{0.21}$	$1.96_{0.57}$	27	$2.31_{0.34}$	$3.78_{0.94}$	23	$2.97_{1.67}$	$3.70_{1.44}$
	13	100	$1.00_{0.02}$	$1.00_{0.02}$	88	$1.26_{0.26}$	$1.86_{0.80}$	37	$1.35_{0.24}$	$2.07_{0.62}$	25	$2.66_{0.46}$	$4.54_{1.07}$	21	$3.16_{1.41}$	$4.44_{1.77}$
20×20	1	100	$1.01_{0.05}$	$1.00_{0.03}$	100	$1.15_{0.17}$	$1.11_{0.13}$	89	$1.14_{0.16}$	$1.14_{0.14}$	40	$1.07_{0.16}$	$1.07_{0.14}$	20	$1.07_{0.18}$	$1.04_{0.12}$
	8	100	$1.00_{0.00}$	$1.00_{0.01}$	100	$1.15_{0.10}$	$1.36_{0.25}$	2	N/A	N/A	1	N/A	N/A	0	N/A	N/A
	10	100	$1.00_{0.01}$	$1.00_{0.02}$	100	$1.26_{0.20}$	$1.64_{0.59}$	1	N/A	N/A	0	N/A	N/A	2	N/A	N/A
	16	100	$1.00_{0.01}$	$1.00_{0.01}$	100	$1.16_{0.10}$	$1.59_{0.33}$	0	N/A	N/A	0	N/A	N/A	0	N/A	N/A
	20	100	$1.01_{0.08}$	$1.00_{0.03}$	99	$1.24_{0.18}$	$1.80_{0.73}$	0	N/A	N/A	0	N/A	N/A	1	N/A	N/A
	24	100	$1.00_{0.02}$	$1.00_{0.00}$	100	$1.18_{0.10}$	$1.81_{0.36}$	0	N/A	N/A	0	N/A	N/A	0	N/A	N/A
	30	100	$1.02_{0.10}$	$1.00_{0.03}$	93	$1.21_{0.19}$	$1.89_{0.66}$	0	N/A	N/A	0	N/A	N/A	2	N/A	N/A
	32	100	$1.00_{0.02}$	$1.00_{0.00}$	100	$1.20_{0.11}$	$1.97_{0.47}$	0	N/A	N/A	0	N/A	N/A	0	N/A	N/A
	40	100	$1.02_{0.12}$	$1.00_{0.02}$	90	$1.20_{0.18}$	$2.05_{0.77}$	0	N/A	N/A	0	N/A	N/A	1	N/A	N/A
	50	100	$1.03_{0.22}$	$1.00_{0.03}$	78	$1.14_{0.15}$	$2.03_{0.84}$	0	N/A	N/A	0	N/A	N/A	1	N/A	N/A
40×40	1	100	$1.02_{0.06}$	$1.01_{0.03}$	100	$1.17_{0.18}$	$1.12_{0.12}$	45	$1.11_{0.14}$	$1.11_{0.12}$	18	N/A	N/A	0	N/A	N/A
	16	100	$1.00_{0.00}$	$1.00_{0.01}$	100	$1.13_{0.10}$	$1.33_{0.22}$	0	N/A	N/A	0	N/A	N/A	0	N/A	N/A
	32	100	$1.00_{0.00}$	$1.00_{0.00}$	100	$1.15_{0.07}$	$1.57_{0.33}$	0	N/A	N/A	0	N/A	N/A	0	N/A	N/A
	40	100	$1.03_{0.18}$	$1.01_{0.04}$	100	$1.13_{0.12}$	$1.51_{0.50}$	0	N/A	N/A	0	N/A	N/A	0	N/A	N/A
	48	100	$1.00_{0.00}$	$1.00_{0.02}$	100	$1.16_{0.08}$	$1.69_{0.33}$	0	N/A	N/A	0	N/A	N/A	0	N/A	N/A
	64	100	$1.00_{0.01}$	$1.00_{0.00}$	100	$1.15_{0.08}$	$1.83_{0.35}$	0	N/A	N/A	0	N/A	N/A	0	N/A	N/A
	80	100	$1.04_{0.31}$	$1.01_{0.10}$	98	$1.12_{0.11}$	$1.79_{0.54}$	0	N/A	N/A	0	N/A	N/A	0	N/A	N/A
	120	100	$1.12_{1.08}$	$1.04_{0.30}$	89	$1.06_{0.10}$	$1.75_{0.62}$	0	N/A	N/A	0	N/A	N/A	0	N/A	N/A
	160	98	$1.10_{0.96}$	$1.03_{0.29}$	72	$1.03_{0.06}$	$1.78_{0.59}$	0	N/A	N/A	0	N/A	N/A	0	N/A	N/A
	200	95	$1.08_{0.23}$	$1.01_{0.07}$	60	$1.02_{0.06}$	$1.81_{0.77}$	0	N/A	N/A	0	N/A	N/A	0	N/A	N/A
80×80	1	100	$1.01_{0.05}$	$1.00_{0.02}$	100	$1.13_{0.14}$	$1.10_{0.10}$	14	N/A	N/A	0	N/A	N/A	0	N/A	N/A
	32	100	$1.00_{0.00}$	$1.00_{0.00}$	100	$1.10_{0.08}$	$1.30_{0.20}$	0	N/A	N/A	0	N/A	N/A	0	N/A	N/A
	64	100	$1.00_{0.00}$	$1.00_{0.00}$	100	$1.11_{0.06}$	$1.41_{0.23}$	0	N/A	N/A	0	N/A	N/A	0	N/A	N/A
	96	100	$1.00_{0.00}$	$1.00_{0.00}$	100	$1.11_{0.06}$	$1.49_{0.23}$	0	N/A	N/A	0	N/A	N/A	0	N/A	N/A
	128	90	$1.00_{0.00}$	$1.00_{0.00}$	86	$1.09_{0.06}$	$1.60_{0.35}$	0	N/A	N/A	0	N/A	N/A	0	N/A	N/A
	160	91	$1.01_{0.03}$	$1.00_{0.02}$	68	$1.04_{0.06}$	$1.43_{0.48}$	0	N/A	N/A	0	N/A	N/A	0	N/A	N/A
	320	90	$1.06_{0.09}$	$1.01_{0.05}$	94	$1.01_{0.02}$	$1.46_{0.41}$	0	N/A	N/A	0	N/A	N/A	0	N/A	N/A
	480	90	$1.10_{0.15}$	$1.01_{0.03}$	75	$1.00_{0.01}$	$1.39_{0.42}$	0	N/A	N/A	0	N/A	N/A	0	N/A	N/A
	640	90	$1.10_{0.18}$	$1.01_{0.07}$	56	$1.00_{0.00}$	$1.40_{0.46}$	0	N/A	N/A	0	N/A	N/A	0	N/A	N/A
	800	80	$1.13_{0.22}$	$1.03_{0.09}$	49	$1.00_{0.00}$	$1.24_{0.33}$	0	N/A	N/A	0	N/A	N/A	0	N/A	N/A
Goal B		100	$1.01_{0.03}$	$1.00_{0.03}$	97	$1.13_{0.14}$	$1.37_{0.44}$	56	$1.20_{0.21}$	$1.45_{0.46}$	49	$1.49_{0.47}$	$1.94_{1.05}$	45	$1.51_{0.88}$	$1.89_{1.28}$
Goal R1		98	$1.02_{0.34}$	$1.01_{0.10}$	82	$1.27_{0.29}$	$1.63_{0.74}$	33	$1.29_{0.28}$	$1.51_{0.64}$	22	$1.35_{0.33}$	$1.46_{0.62}$	22	$1.45_{0.82}$	$1.71_{1.16}$
Goal R2		99	$1.02_{0.10}$	$1.01_{0.04}$	100	$1.16_{0.22}$	$1.42_{0.52}$	56	$1.29_{0.27}$	$1.56_{0.61}$	47	$1.53_{0.48}$	$1.85_{1.02}$	44	$1.57_{0.76}$	$1.96_{1.35}$
All		99	$1.02_{0.21}$	$1.01_{0.06}$	93	$1.18_{0.23}$	$1.46_{0.59}$	48	$1.26_{0.26}$	$1.51_{0.57}$	39	$1.48_{0.46}$	$1.81_{1.00}$	37	$1.52_{0.82}$	$1.88_{1.29}$

Table 7: Average fist versus final solution cost ratio for *LaCAM*-based MAPF approach, grouped by the number of grid size (GS), number of target blocks (TB), and goal types.

Groups		Succ. Rate	First Comp. Cost	Final Comp. Cost	First Sol. Time (ms)
GS	TB				
4×10	1	100	$1.14_{0.24}$	$1.00_{0.03}$	$0.2_{0.0}$
	2	100	$1.25_{0.33}$	$1.00_{0.02}$	$0.2_{0.1}$
	3	100	$1.36_{0.47}$	$1.00_{0.03}$	$0.2_{0.1}$
	4	100	$1.49_{0.66}$	$1.00_{0.02}$	$0.3_{0.1}$
	5	100	$1.55_{0.71}$	$1.01_{0.05}$	$0.3_{0.1}$
	6	100	$1.64_{1.11}$	$1.00_{0.02}$	$0.3_{0.2}$
6×10	1	100	$1.15_{0.22}$	$1.01_{0.05}$	$0.2_{0.1}$
	2	100	$1.20_{0.28}$	$1.01_{0.05}$	$0.2_{0.1}$
	3	100	$1.34_{0.40}$	$1.01_{0.03}$	$0.3_{0.1}$
	5	100	$1.46_{0.45}$	$1.01_{0.03}$	$0.4_{0.2}$
	6	100	$1.52_{0.45}$	$1.00_{0.03}$	$0.4_{0.2}$
	8	100	$1.62_{0.52}$	$1.00_{0.01}$	$0.5_{0.3}$
8×10	1	100	$1.14_{0.23}$	$1.01_{0.04}$	$0.3_{0.1}$
	2	100	$1.21_{0.25}$	$1.01_{0.03}$	$0.4_{0.1}$
	4	100	$1.34_{0.33}$	$1.01_{0.03}$	$0.5_{0.2}$
	6	100	$1.38_{0.35}$	$1.01_{0.03}$	$0.6_{0.3}$
	8	100	$1.51_{0.44}$	$1.00_{0.02}$	$0.7_{0.4}$
	10	100	$1.58_{0.49}$	$1.00_{0.02}$	$0.9_{0.6}$
10×10	1	100	$1.14_{0.24}$	$1.01_{0.04}$	$0.4_{0.1}$
	3	100	$1.27_{0.41}$	$1.01_{0.03}$	$0.5_{0.2}$
	5	100	$1.33_{0.28}$	$1.01_{0.02}$	$0.7_{0.3}$
	8	100	$1.45_{0.38}$	$1.00_{0.02}$	$0.9_{0.5}$
	10	100	$1.55_{0.41}$	$1.00_{0.01}$	$1.1_{0.6}$
	13	100	$1.64_{0.54}$	$1.00_{0.02}$	$1.4_{1.1}$
20×20	1	100	$1.15_{0.22}$	$1.01_{0.05}$	$2.3_{1.0}$
	8	100	$1.12_{0.08}$	$1.00_{0.00}$	$3.8_{1.9}$
	10	100	$1.37_{0.29}$	$1.00_{0.01}$	$5.9_{5.7}$
	16	100	$1.16_{0.09}$	$1.00_{0.01}$	$5.5_{3.7}$
	20	100	$1.41_{0.35}$	$1.01_{0.08}$	$8.7_{11.2}$
	24	100	$1.20_{0.11}$	$1.00_{0.02}$	$7.9_{6.7}$
	30	100	$1.48_{0.54}$	$1.02_{0.10}$	$12.6_{20.6}$
	32	100	$1.26_{0.12}$	$1.00_{0.02}$	$10.8_{10.5}$
	40	100	$1.43_{0.52}$	$1.02_{0.12}$	$15.8_{24.4}$
	50	100	$1.62_{1.01}$	$1.03_{0.22}$	$26.2_{55.8}$
40×40	1	100	$1.14_{0.14}$	$1.02_{0.06}$	$19.6_{9.1}$
	16	100	$1.07_{0.04}$	$1.00_{0.00}$	$36.4_{32.4}$
	32	100	$1.09_{0.05}$	$1.00_{0.00}$	$55.3_{70.0}$
	40	100	$1.25_{0.45}$	$1.03_{0.18}$	$96.2_{203.4}$
	48	100	$1.11_{0.05}$	$1.00_{0.00}$	$79.2_{121.1}$
	64	100	$1.14_{0.07}$	$1.00_{0.01}$	$105.8_{178.6}$
	80	100	$1.25_{0.57}$	$1.04_{0.31}$	$169.3_{429.2}$
	120	100	$1.36_{1.27}$	$1.12_{1.08}$	$351.0_{1062.4}$
	160	98	$1.35_{1.39}$	$1.10_{0.96}$	$437.1_{1429.0}$
	200	95	$1.35_{0.37}$	$1.08_{0.23}$	$285.7_{654.7}$
80×80	1	100	$1.12_{0.12}$	$1.01_{0.05}$	$206.8_{87.9}$
	32	100	$1.03_{0.02}$	$1.00_{0.00}$	$456.4_{577.9}$
	64	100	$1.04_{0.02}$	$1.00_{0.00}$	$747.9_{1374.2}$
	96	100	$1.04_{0.03}$	$1.00_{0.00}$	$1085.7_{2247.0}$
	128	90	$1.07_{0.04}$	$1.00_{0.00}$	$541.7_{908.8}$
	160	91	$1.12_{0.13}$	$1.01_{0.03}$	$627.4_{764.9}$
	320	90	$1.13_{0.10}$	$1.06_{0.09}$	$979.5_{558.8}$
	480	90	$1.16_{0.16}$	$1.10_{0.15}$	$1914.2_{1290.7}$
	640	90	$1.15_{0.19}$	$1.10_{0.18}$	$3141.1_{2136.6}$
	800	80	$1.17_{0.25}$	$1.13_{0.22}$	$4290.4_{2766.3}$
Goal B		100	$1.19_{0.23}$	$1.01_{0.03}$	$98.1_{515.0}$
Goal R1		98	$1.44_{0.72}$	$1.02_{0.34}$	$393.7_{1323.4}$
Goal R2		99	$1.31_{0.44}$	$1.02_{0.10}$	$141.3_{492.5}$
All		99	$1.31_{0.52}$	$1.02_{0.21}$	$210.2_{875.0}$

Table 8: Average first versus final solution cost ratio for *LaCAM*-based MAPF approach on instances with distinct goal location sets for each target block, grouped by the number of grid size (GS) and number of target blocks (TB).

Groups		Succ. Rate	First Comp. Cost	Final Comp. Cost	First Sol. Time (ms)
GS	TB				
4×10	1	100	$1.10_{0.29}$	$1.00_{0.00}$	$0.1_{0.0}$
	2	100	$1.24_{0.36}$	$1.00_{0.00}$	$0.2_{0.0}$
	3	100	$1.29_{0.36}$	$1.00_{0.00}$	$0.2_{0.1}$
	4	100	$1.39_{0.47}$	$1.00_{0.00}$	$0.2_{0.1}$
	5	100	$1.58_{0.83}$	$1.00_{0.00}$	$0.3_{0.1}$
	6	100	$1.65_{0.49}$	$1.00_{0.00}$	$0.3_{0.1}$
6×10	1	100	$1.12_{0.27}$	$1.00_{0.00}$	$0.2_{0.0}$
	2	100	$1.20_{0.26}$	$1.00_{0.00}$	$0.2_{0.1}$
	3	100	$1.31_{0.32}$	$1.00_{0.00}$	$0.3_{0.1}$
	5	100	$1.37_{0.45}$	$1.00_{0.00}$	$0.3_{0.1}$
	6	100	$1.52_{0.50}$	$1.00_{0.00}$	$0.4_{0.1}$
	8	100	$1.66_{0.43}$	$1.00_{0.00}$	$0.5_{0.2}$
8×10	1	100	$1.13_{0.21}$	$1.00_{0.00}$	$0.2_{0.1}$
	2	100	$1.19_{0.31}$	$1.00_{0.00}$	$0.3_{0.1}$
	4	100	$1.31_{0.23}$	$1.00_{0.00}$	$0.4_{0.1}$
	6	100	$1.40_{0.34}$	$1.00_{0.00}$	$0.5_{0.2}$
	8	100	$1.51_{0.38}$	$1.00_{0.00}$	$0.7_{0.4}$
	10	100	$1.63_{0.41}$	$1.00_{0.00}$	$0.8_{0.5}$
10×10	1	100	$1.16_{0.30}$	$1.00_{0.00}$	$0.3_{0.1}$
	3	100	$1.24_{0.22}$	$1.00_{0.00}$	$0.5_{0.1}$
	5	100	$1.31_{0.25}$	$1.00_{0.00}$	$0.6_{0.2}$
	8	100	$1.45_{0.38}$	$1.00_{0.00}$	$0.8_{0.4}$
	10	100	$1.52_{0.38}$	$1.00_{0.00}$	$1.0_{0.6}$
	13	100	$1.61_{0.35}$	$1.00_{0.00}$	$1.3_{0.9}$
20×20	1	100	$1.11_{0.16}$	$1.00_{0.00}$	$1.6_{0.6}$
	10	100	$1.25_{0.13}$	$1.00_{0.00}$	$5.3_{3.8}$
	20	100	$1.26_{0.11}$	$1.00_{0.00}$	$8.9_{8.9}$
	30	100	$1.29_{0.15}$	$1.00_{0.00}$	$13.8_{17.3}$
	40	100	$1.29_{0.13}$	$1.00_{0.00}$	$20.4_{32.3}$
	50	100	$1.28_{0.13}$	$1.00_{0.00}$	$27.3_{45.7}$
40×40	1	100	$1.14_{0.13}$	$1.00_{0.00}$	$15.0_{5.8}$
	40	100	$1.11_{0.06}$	$1.00_{0.00}$	$98.7_{160.5}$
	80	100	$1.10_{0.04}$	$1.00_{0.00}$	$196.2_{387.2}$
	120	100	$1.09_{0.04}$	$1.00_{0.00}$	$347.1_{765.9}$
	160	100	$1.08_{0.04}$	$1.00_{0.00}$	$490.3_{1114.2}$
	200	100	$1.06_{0.04}$	$1.00_{0.00}$	$783.4_{1927.8}$
80×80	1	100	$1.13_{0.10}$	$1.00_{0.00}$	$142.1_{44.1}$
	160	91	$1.03_{0.01}$	$1.00_{0.00}$	$692.6_{141.3}$
	320	91	$1.02_{0.01}$	$1.00_{0.00}$	$1193.8_{448.2}$
	480	91	$1.02_{0.01}$	$1.00_{0.00}$	$1819.3_{853.7}$
	640	91	$1.01_{0.01}$	$1.00_{0.00}$	$2796.0_{1731.0}$
	800	82	$1.01_{0.01}$	$1.00_{0.00}$	$3246.2_{1652.4}$
All		99	$1.26_{0.37}$	$1.00_{0.00}$	$258.8_{853.2}$